Contrib Mineral Petrol (1996) 126: 199 – 215

M.B. Fowler · P.J. Henney

Mixed Caledonian appinite magmas: implications for lamprophyre fractionation and high Ba-Sr granite genesis

Received: 26 September 1995 / Accepted: 5 June 1996

Abstract Ach'Uaine Hybrid appinites represent a rare example of lamprophyric magmas that were demonstrably exactly contemporaneous with felsic differentiates, preserved within a suite of minor, hypabyssal intrusions emplaced at the end of the Caledonian orogeny in northern Scotland. Numerous small stocks, bosses and dykes show outcrop-scale relationships characteristic of mingling between lamprophyric and syenitic magmas, and are commonly cut by sharp-sided granite veins. The mafic rocks are characterised by Ni and Cr abundances and MgO sufficiently high to signal derivation from a mantle source within which radiogenic $^{87}Sr/^{86}Sr$ and nonradiogenic $^{143}Nd/^{144}Nd$ ratios require significant time-integrated incompatible element enrichment. This is manifest in high Ba, Sr and light REE abundances and incompatible element ratios in the derived magmas directly comparable with those of high Ba-Sr granitoids and related rocks. Quantitative major element, trace element, radiogenic and stable isotope modelling is consistent with early fractionation of clinopyroxene and biotite, accompanied by minor crustal assimilation, having driven the evolving lamprophyric magma to cogenetic syenite. Subsequent derivation of granite required a major change to feldspar-dominated crystal fractionation with continued, still minor contamination. The elemental and isotopic characteristics of the granitic terminus are so similar to high Ba-Sr granitoids both locally and worldwide, that these too may have had large mantle components and represent significant juvenile additions to the crust.

M. B. Fowler (✉)
Division of Geology and Cartography,
Oxford Brookes University,
Headington, Oxford OX3 0BP,
U.K.

P. J. Henney
British Geological Survey, Keyworth,
Nottingham NG12 5GG, U.K.

Editorial responsibility: T. Grove

Introduction

Many recent publications explore the significance of volumetrically minor lamprophyric magmatism, in a variety of geodynamic settings (e.g. Allan and Carmichael 1984; Leat et al. 1987; Wallace and Carmichael 1989, Stille et al. 1989, Thompson et al. 1989; Gibson et al. 1993; Canning et al. 1996). However, only a little work has been published on the mechanisms of lamprophyre fractionation. Roden (1981) related felsic minettes (60 wt% SiO_2, 5 wt% MgO) of the Buell Park diatreme, Navajo volcanic field, Arizona directly to closely-associated mafic minette (49 wt% SiO_2, 10 wt% MgO) by crystal fractionation accompanied by crustal contamination. Esperança and Holloway (1986, 1987) investigated the experimental melting relationships of the same rocks, closely constraining the minerals involved in high pressure fractional crystallisation and confirming the possible production of a series of potassic daughter liquids during ascent (potassic latites and felsic minettes). More recently, Wyman and Kerrich (1993) and Wyman et al. (1995) related variations in elemental abundances and isotopic ratios to a variety of processes including melting of heterogeneous sources, assimilation - fractional crystallisation and magma mixing. Finally, Righter and Carmichael (1996) formulated thermobarometric expressions for lamprophyric compositions and related felsic minettes to mafic minettes by simple fractionation, on the basis of derived *PT* estimates, experimental work and major element modelling.

The Ach'Uaine appinites (Fowler 1988a) represent a rare example where lamprophyric magmas were demonstrably exactly contemporaneous with silica-oversaturated felsic differentiates. The present contribution describes this mixed-magma complex and presents new elemental and Nd, Sr, O isotope data, drawing significant conclusions about fractionation mechanisms of lamprophyric magma to syenite and granite, with attendant implications for the petrogenesis of high Ba-Sr

granites in general and British Caledonian Newer Granites in particular.

Appinites and associated lamprophyres are a characteristic feature of British Caledonian magmatism, but have received little attention in a region dominated by granite and syenite intrusions. The granite plutons have formed the subject of protracted and well-known research (e.g. Harmon et al. 1984; Stephens and Halliday 1984). Tarney and Jones (1994) used the granites in the west of Scotland as type examples of their HiBaSr class, regarded as distinct from traditional I-type, S-type and A-type granites on the basis of a range of geochemical characteristics including high Ba, Sr, K/Rb, and low Rb, Th, U, Nb, Y and heavy rare earth elements (HREE). Recent work on the syenites (Fowler 1988b, 1992; Thirlwall and Burnard 1990) emphasises the control of crystal-liquid equilibria during magma evolution and recognises the influence of crustal contamination if a silica-oversaturation trend is present. Thompson and Fowler (1986) noted the elemental similarities between the mafic parts of the syenite complexes and spatially-associated, broadly coeval lamprophyres, suggesting that the latter may represent mantle-derived parent magma of the former. Fowler (1988a) drew these strands together by suggesting that the composite lamprophyre/syenite/granite Ach'Uaine Hybrid appinites represent in microcosm the same evolutionary sequence as the discrete lamprophyre dykes, syenite and granite plutons, but in this case derived from a petrologically-complex and evolving Caledonian magma chamber (cf. Platten 1991). Finally, Rock and Hunter (1987) studied composite dykes of lamprophyre and microgranitic porphyry in the environs of the Caledonian Ross of Mull pluton, concluding that their relationship was genetic and that lamprophyric magma probably had a significant role in the genesis of the granite itself.

Appinites

The appinite suite of the Scottish Highlands comprises a group of of ultramafic to intermediate minor intrusions intruded during the final stages of the Caledonian orogeny (Bowes and McArthur 1976; Wright and Bowes 1979; Hamidullah and Bowes 1987). They are most commonly found as small stocks, bosses, sheets and dykes and are often associated closely with late-post tectonic granitoid intrusions. The most distinctive facies of the suite is a coarse grained hornblende meladiorite, often porphyritic, with phenocrysts of brown or green hornblende set in a feldspathic groundmass commonly comprising equal proportions of plagioclase and K-feldspar. Other lithologies include hornblende peridotites (cortlandite), phlogopite-bearing picrites (kentallenite), hornblendites, hornblende gabbros and a variety of hornblende-clinopyroxene-biotite bearing meladiorites. The most evolved compositions include leucodiorites, granodiorites and more rarely biotite granites, and a large variety of felsic segregations, globular structures and veins containing varying proportions of K-feldspar, acid plagioclase, quartz and carbonate also occur as irregular masses within all facies. The intrusive relationships betwen the different phases are often complex with evidence for multiple intrusion and remobilisation as well as in-situ differentiation and complex interactions with the surrounding country rocks, including local partial melting (Hamidullah and Bowes 1987; Platten 1991). Geochemically, the appinite suite is characterised by generally high Ni, Cr, V and MgO values coupled with elevated large ion lithophile element (LILE) and light rare earth element (LREE) abundances, and with high $Na_2O + K_2O$ together with K_2O/Na_2O generally ≥ 1. With respect to high field strength elements (HFSE), it also shows the high LILE/HFSE and LREE/HFSE ratios characteristic of subduction-related magmas, and the parent magma is considered to derive from subduction-modified mantle (Wright and Bowes 1979; Hamidullah and Bowes 1987; Fowler 1988a). Rock (1984, 1991) pointed out that many of the more primitive members of the appinite suite have close similarities in petrography, mineral chemistry and whole-rock geochemistry with calc-alkaline lamprophyres, and accepted the suite to represent the plutonic equivalent of spessartites and vogesites. In this contribution, the nomenclature recommendations of Middlemost (1994) are followed, using the plutonic TAS diagram (Fig. 1).

Ach'Uaine Hybrid appinites

MacGregor and Kennedy (1932) first proposed a correlation between accepted appinites on the Ardgour peninsula near the Strontian Newer Granite and the so-called Ach'Uaine Hybrids (Read et al. 1926) of Sutherland. These were originally described from a locality near Loch Scye, from which the term "scyelite" was coined for a phlogopite-bearing hornblende-peridotite. They form a complete series from such ultramafic rock types through to felsic varieties, linked by the ubiquitous presence of alkali feldspar. The hypothesis of Read et al. (1926) related intermediate rock types to the end members by a process of magmatic hybridisation.

In the vicinity of the Migdale Newer Granite, forty or so small masses of such appinite are known (Fig. 2). The largest of this group is the body at Ach'Uaine, 4 km NNE of Bonar Bridge, from which the whole suite took its name. Samples used in this study are from this and the neighbouring cluster at Lydsurach - Cnoc a Choire Bhuidhe. The latter forms a small swarm of cross-cutting minor intrusions with a general NW-SE trend, only 0.5km in maximum length.

Field relationships

The Ach'Uaine appinites are clustered together as groups of elongate bodies, the sense of elongation coinciding with the structural fabric of the surrounding Proterozoic Moine metasedimentary rocks. As is typical in Sutherland, the appinites are poorly

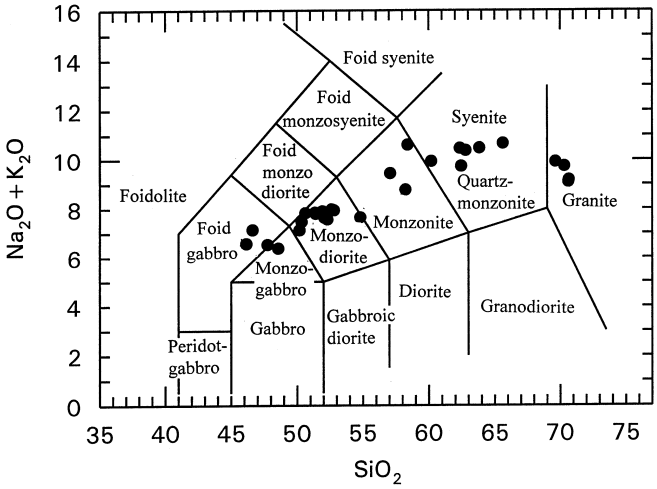

Fig. 1 Lithological nomenclature for the Ach'Uaine Hybrid Appinites on the basis of the plutonic TAS diagram of Middlemost (1994)

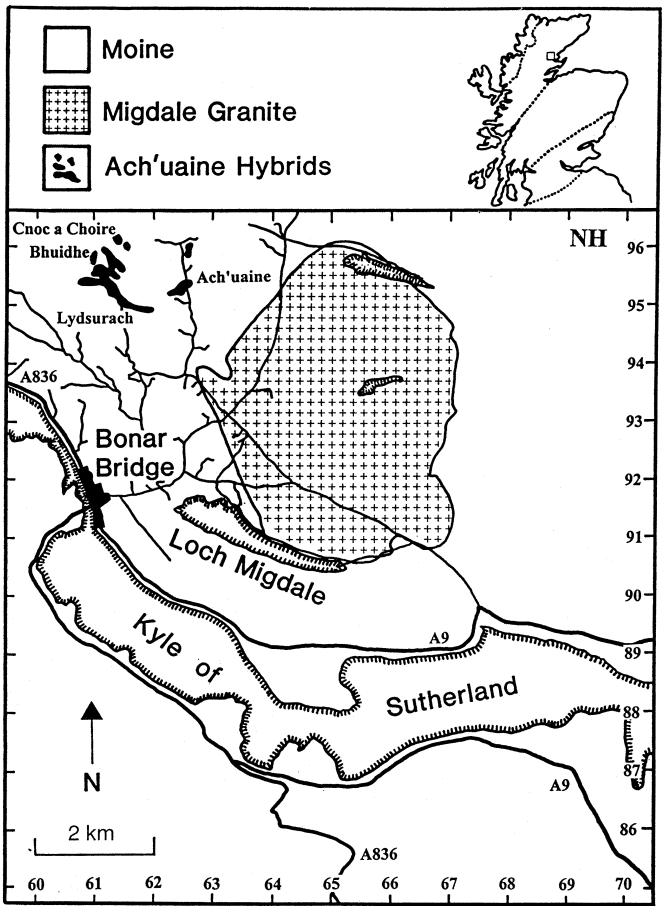

Fig. 2 Locality map for the Ach'Uaine Hybrid appinites – a suite of minor intrusions spatially and temporally associated with the Migdale Newer Granite, north of Bonar Bridge in the Northern Highlands of Scotland

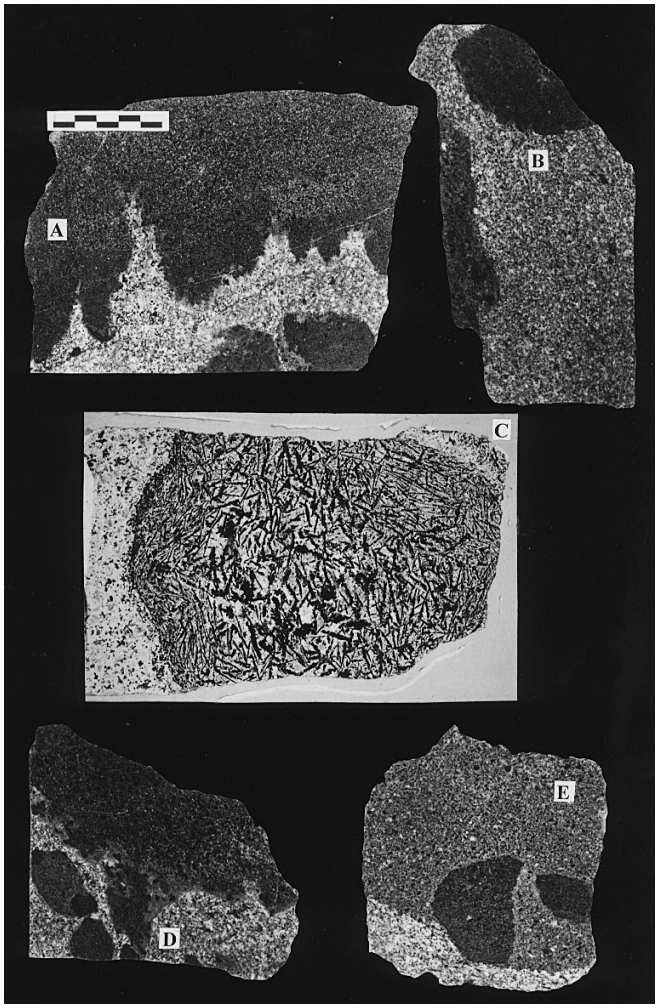

Fig. 3A–E Relationships between monzodiorite and syenite: **A** Flames of syenite invading monzodiorite. **B** Crenulate contact of monzodiorite pillow with syenite host. **C** Biotite aligned tangential to contact (thin section). **D** Plucking of fine-grained monzodiorite inclusions from pillow margins. **E** Intimate mixing producing genuine hybrid. Scale for A, B, D and E is the same, scale bar divisions are centimetres; base of view C (thin section) represents 4 centimetres

exposed. They are undeformed, and their margins are sharp but rarely chilled. Local recrystallisation (< 10 cm) of the psammitic country rocks has occured, occasionally accompanied by feldspathisation and amphibole growth. Xenoliths of Moine metasediments are common, showing variable reaction with the appinite magma. The intrusions exposed at Cnoc a Choire Bhuidhe show many features attributable to mingling and mixing between mafic and felsic magmas (Fig. 3). For example, flames of syenite invading monzodiorite pillows (Fig. 3A), crenulate enclaves of monzodiorite in syenite (Fig. 3B, cf. Marshall and Sparks 1984; D'Lemos 1992), marginal biotite crystals aligned tangential to the enclave contact (Fig. 3C), monzodiorite inclusions with chilled margins, and small (1 cm) quenched inclusions (Fig. 3D). These features are sufficient to confirm the former coexistence of two liquids (Vernon 1991). Finally, intimate mixing has clearly sometimes occurred between the inclusions and their syenitic host (Fig. 3E). After emplacement as small, hypabyssal intrusions, during which the mingling likely occurred, the complex was cut by many thin (10 cm) sharp-sided granite veins, probably derived from the nearby Migdale Newer Granite. These frequently contain clots of biotite reminiscent of the small, quenched inclusions in the syenites.

Petrography

Four rock types dominate the sporadic exposures of the Ach'Uaine appinites (Fig. 1). The most mafic is a coarse-grained monzogabbro, forming many of the bosses, small stocks and dykes. It is composed of large, ragged plates of light green-brown biotite, associated with poorly-formed often zoned diopsidic clinopyroxene, both set in a matrix of anhedral sodic plagioclase and alkali feldspar. Amphibole is present in small and variable amounts at the expense of pyroxene. Minor titanite and apatite are conspicuous as euhedral grains scattered throughout the rock-forming minerals. Iron-titanium oxides and rutile are ubiquitous accessories, and a few large plates of carbonate are also present. Distinguishable from this rock type, but with gradation between the two, is that which forms the abundant mafic inclusions in the mixed-magma complex. This is a medium-grained biotite-, pyroxene- and amphibole-bearing monzodiorite. Its amphibole content is higher than in the monzogabbros, the biotite is less conspicuous, and sodic plagioclase dominates alkali feldspar. However, both the feldspars often display a well-developed granoblastic texture, which is similar to that often seen in synplutonic dykes (Pitcher 1993). All stages of transformation to the granular overprint may be observed. Accessory phases include abundant titanite and apatite, and minor allanite. The leucocratic host of such monzodiorite inclusions has abundant, commonly sericitised plagioclase phenocrysts that usually show complex zonation, corrosion and overgrowth tex-

tures. These are often mantled in-situ by alkali feldspar or moresodic plagioclase. Quartz is rare. Such syenites contain amphibole and biotite but little pyroxene, together with abundant magnetite plus accessory allanite, titanite, zircon and apatite. Granular microtextures are less common than in the monzodiorites. Finally, the late, cross-cutting granite dykes are medium-grained biotite-bearing microgranites with plagioclase phenocrysts displaying textures similar to those in the syenites. Biotite is occasionally chloritised, and sericitisation of feldspar is common. Tiny, accessory zircon and titanite crystals are abundant, allanite and apatite less so.

Certain petrographic features of all the main rock types are consistent with the former presence of discrete, coexisting magmas that mixed and mingled at several stages of their evolution. In particular, the corroded, zoned and mantled plagioclase phenocrysts that characterise the syenite, and to a lesser extent the granite dykes, are consistent with multiple mixing events in the magma before its emplacement at the present level of exposure. Occasionally, such feldspar phenocrysts are found within the monzodiorite pillows where they represent phenocryst transfer from felsic to mafic magma. More commonly, mafic schlieren are scattered in the syenite host, representing transfer of mafic material into felsic magma. In rare cases, such two-way material transfer proceeded to extreme, and localised genuine hybrid rocks were produced.

Sampling and analytical techniques

Forty samples, many of them composite, were collected to represent the range of rock types exposed. Care was taken during preparation to ensure that analyses presented derive from internally homogeneous, single lithologies. Samples were crushed in a tungsten carbide shatterbox to pass 200#, and analysed by the following techniques:

Major elements were determined by Inductively Coupled Plasma Atomic Emission Spectrometry (ICPAES) at Imperial College (IC) and Oxford Brookes University by fusion dissolution followed by analysis against calibrations defined with international standard rock materials (SRMs). Accuracy and precision are estimated to be better than 2–3% relative standard deviation (rsd), on the basis of SRM analytical results and precision tests. Rare earth elements were also determined by ICPAES, following cation-exchange preconcentration, at IC and Kings College, London. Synthetic multielement rare earth standards were used, following the methodology of Walsh et al. (1981). Rubidium, Sr, Ba, Y, Zr, Nb, V, Cr, Co, Ni, Cu and Zn were determined by X-ray Fluorescence Spectrometry (XRF) at the British Geological Survey (BGS), again calibrated and assessed with international SRMs. Uranium, Th, Ta and Hf were determined by Instrumental Neutron Activation Analysis (INAA) at the University of Munich. Accuracy and precision of all the trace element analyses are better than 5% rsd, estimated as for the major element determinations.

Mineral analyses were obtained at the BGS using a Cameca SX50 wavelength dispersive electron probe with an accelerating voltage of 15 kV and a beam current of 20nA. Calibrations used a range of appropriate synthetic and natural materials. Accuracy and precision of these analyses are estimated to be better than 3% rsd.

Oxygen isotope analyses were performed using fluorination techniques based on those of Clayton and Mayeda (1963). Six to ten milligrams of whole-rock powder were reacted with BrF_5 at 550 °C for 16 h, following overnight outgassing at 250 °C in vaccuo and prefluorination for 2 h at room temperature. Oxygen thus liberated was converted to CO_2 by Pt-catalysed reaction with heated graphite, and the CO_2 samples analysed on a VG Isogas Sira 10 triple collector mass spectrometer, at the NERC Isotope Geosciences Laboratory (NIGL). Measured $^{18}O/^{16}O$ ratios are reported in standard delta notation relative to V-SMOW, and are estimated to be within 0.2‰ of the true value, on the basis of international and in-house standard analyses, and replicate determinations. International quartz standard NBS 28 gave a $\delta^{18}O$ value of +9.6‰ throughout the period of analysis.

Neodymium and Sr for isotopic analysis were separated from whole-rock powders by standard cation exchange procedures following HF/HNO_3 dissolution. Isotopic analyses were performed at NIGL using a VG 354 automated thermal ionisation mass spectrometer. Determinations on international standards covering the period during which the analyses were made are as follows: La Jolla $^{143}Nd/^{144}Nd = 0.511827 \pm 30$ ppm (2σ), n = 47; NBS 987 $^{87}Sr/^{86}Sr = 0.710221 \pm 54$ ppm (2σ), n = 54.

Whole-rock geochemistry

Whole rock elemental and isotopic data (Table 1) are used below to address three main issues: the tectonomagmatic affinities of the magmas, the mechanisms of lamprophyre differentiation, and the identity and nature of the source region(s).

Elemental abundances

The range of compositions (Table 1) is extensive, with SiO_2 varying between 46.2 and 70.7% and MgO between 9.4 and 0.1%. Monzogabbros and monzodiorites have MgO (up to ca. 10% by weight) and transition metal abundances (Cr up to 585 ppm and Ni up to 163 ppm) sufficiently high to require derivation from the mantle. Several characteristic elemental features persist throughout the suite – for example high Ba, Sr, K_2O, Na_2O and high La/Yb ratios (fractionated rare earth element patterns). Each of these is a feature of the shoshonite association of subduction-related magmas (Morrison 1980). The Ach'Uaine appinites thus represent intrusive products of Caledonian shoshonitic magmatism in N Scotland (Fowler 1988b), in common with the syenites (Thompson and Fowler 1986; Thirlwall and Burnard 1990), and some of the associated Lorne lavas (Thirlwall 1982).

It has become increasingly clear as studies of magma mixing and mingling have progressed, that a severe problem in the interpretation of any geochemical data results from partial or complete equilibration of small enclaves of generally mafic material with their felsic hosts while both are still liquid (e.g. Watson 1982). Recent studies (Holden et al. 1991; Stephens et al. 1991) have shown that in the plutonic environment, elements equilibrate at different rates, controlled dominantly by diffusion. Investigations into disrupted synplutonic dykes indicate that the high field strength elements retain original magmatic concentrations, whereas large-ion lithophile elements may lose useful petrogenetic information by diffusion across the enclave/host contact. However, in the present situation, intimate mixing has occured in subvolcanic conduits relatively close to the surface, so that the time available for chemical equilibration was comparatively short. This suggests that the observed elemental variations may reflect primary magmatic controls.

Three of the four main lithologies occupy distinct fields on Harker diagrams (Fig. 4), but the monzogab-

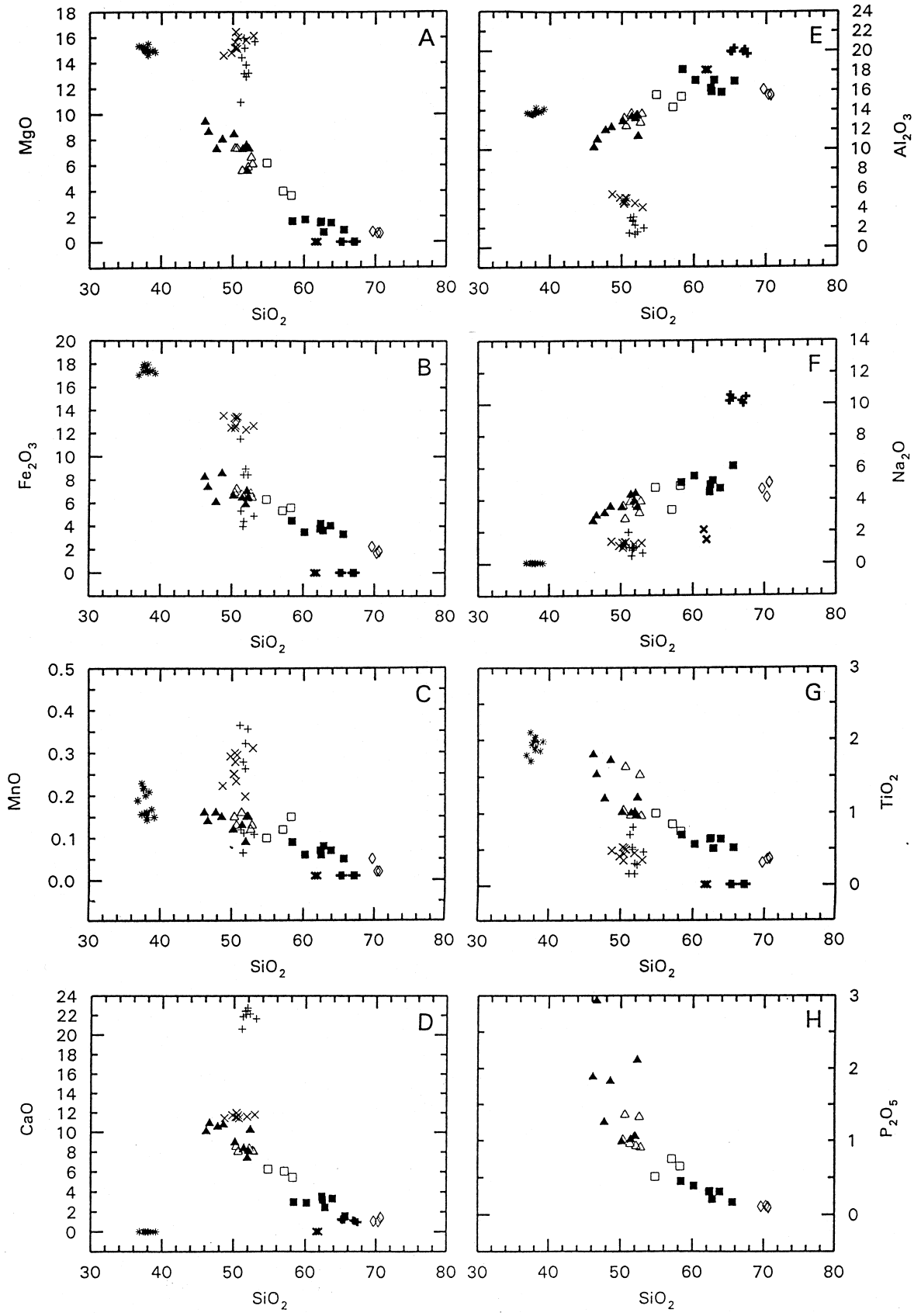

Fig. 4A–H Harker plots for major element oxide data. Rock analyses: *closed triangles* monzogabbros, *open triangles* monzodiorites, *closed squares* syenites, *open squares* genuine hybrids, *open diamonds* granites. Mineral analyses: *asterisks* biotite, + clinopyroxene, × amphibole, *bold*+ = plagioclase, *bold* × K-feldspar

bro field always overlaps with that of the monzodiorites. There are two main types of trend with increasing SiO_2: consistently falling (Fe_2O_3, TiO_2, MgO, CaO, P_2O_5), and concave downwards (Al_2O_3, Na_2O). These clearly relate to the mineralogical affinities of the element groups, namely the ferromagnesian phases (calcic clinopyroxene, amphibole and biotite) and apatite for the former and feldspars for the latter. If the observed trends correspond with the crystallisation sequence from the magmas, crystal fractionation mechanisms are likely to have been responsible. Although the petrography is complicated by the granular overprint, early crystallising minerals in the monzodiorite melt were phlogopitic biotite and clinopyroxene (Mg# 88, where Mg# = [Mg/(Mg+Fe)] × 100), with accessory apatite and titanite. That plagioclase and amphibole joined this assemblage late is shown by the presence of plagioclase phenocrysts (An_{12-14}) and ubiquitous amphibole (Mg# 71–52) only in the syenites, and it is from this point to the granite extreme that the influence of feldspar is recorded in the Harker plots. The major element oxide trends, especially the curvature of Al_2O_3 and Na_2O, may be explained by this switch from biotite- and pyroxene-dominated to feldspar-dominated crystallisation, the former responsible for the monzodiorite to syenite fractionation, the latter for the syenite to granite step. These relation-

Table 1 Whole-rock major element, trace element, stable and radiogenic isotope data for the Ach'Uaine Hybrid appinites (na not analysed)

	A 45	LYD 1	A 49	CCB 2	A 38	CCB 3	CCB 1i	CCB 14	A 56	A 254	A 40	CCB 15	A 34	CCB 16	A 34A
	Monzogabbros and monzodiorities														
SiO_2	46.15	46.62	47.75	48.56	50.17	50.33	50.62	51.34	51.40	51.91	52.06	52.17	52.29	52.61	52.79
Al_2O_3	10.20	10.98	11.94	12.24	12.85	13.19	12.38	13.67	13.35	13.15	13.48	13.49	11.33	12.73	13.63
TiO_2	1.80	1.53	1.20	1.72	1.01	1.04	1.63	0.97	1.00	1.01	0.96	0.97	1.21	1.52	0.96
Fe_2O_3	8.25	7.38	6.08	8.58	6.62	6.91	7.21	6.71	6.44	5.88	7.03	6.39	6.47	6.82	6.47
MnO	0.16	0.14	0.16	0.15	0.12	0.15	0.13	0.16	0.13	0.09	0.15	0.15	0.15	0.12	0.13
MgO	9.41	8.60	7.25	8.00	8.40	7.30	7.29	5.56	7.24	7.53	5.54	5.83	7.28	6.59	6.07
CaO	10.08	10.90	10.54	10.75	8.94	8.52	8.00	8.23	8.33	7.37	8.04	8.30	10.21	8.07	7.99
K_2O	3.93	4.16	3.39	2.84	3.62	3.88	5.06	4.00	3.50	3.98	3.26	4.11	4.07	4.83	4.06
Na_2O	2.64	2.98	3.14	3.54	3.51	3.59	2.77	3.85	4.30	3.92	4.38	3.68	3.50	3.15	3.88
P_2O_5	1.88	2.93	1.25	1.82	0.98	1.01	1.35	0.95	1.01	1.05	1.05	0.92	2.11	1.32	0.90
LOI	3.13	2.97	5.11	0.99	2.97	3.67	1.80	3.39	1.96	2.87	3.53	2.83	1.13	1.90	2.32
TOTAL[a]	98.07	99.83	98.24	99.62	99.82	100.17	98.93	99.43	99.23	99.19	99.94	99.43	100.26	100.26	99.81
Rb	100	105	115	129	93	98	135	97	77	76	84	95	85	95	104
C	na	3.6	na	5.8	na	3.5	na	2.8	na	na	na	na	na	2.8	na
Sr	1306	1964	1966	2432	2026	2023	2060	2255	1930	1686	1893	2246	2230	2017	2360
Ba	2527	3686	1772	1477	3453	3057	3987	2971	3056	2093	2079	2870	2199	3212	2923
Y	34	31	19	31	25	23	32	25	24	20	29	23	32	27	24
Th	25.0	30.5	10.0	35.7	26.0	38.1	32.0	31.6	37.0	25.0	25.0	29.0	23.0	34.5	30.0
U	na	9.0	na	10.4	na	10.8	na	8.4	na	na	na	na	na	9.2	na
Zr	560	398	191	485	254	303	376	312	298	273	327	305	352	419	329
Hf	na	10.5	na	13.5	na	8.5	na	7.5	na	na	na	na	na	11.5	na
Nb	32	30	27	46	21	24	32	24	24	21	19	23	30	30	23
Ta	na	1.9	na	3.2	na	2.1	na	1.5	na	na	na	na	na	2.2	na
V	106	95	95	128	111	109	116	98	103	96	101	99	75	106	98
Cr	585	180	385	186	386	279	247	250	280	99	205	253	294	229	239
Co	31	27	29	27	28	26	25	24	27	30	23	27	24	26	25
Ni	163	116	132	43	88	78	76	74	72	93	62	74	118	63	68
Cu	27	7	41	6	47	5	17	19	40	44	25	23	20	14	12
Zn	126	104	102	139	86	101	111	103	83	131	113	95	109	94	89
La	197.0	187.0	81.9	202.0	187.0	188.0	191.0	183.0	217.0	134.0	216.0	179.0	159.0	170.0	177.0
Ce	437	425	205	472	390	392	410	378	421	285	446	370	385	373	366
Pr	39.0	41.1	23.9	44.8	35.1	36.9	39.1	35.6	37.4	28.0	37.8	34.8	38.3	36.2	33.7
Nd	159	174	96	187	135	145	158	137	143	106	144	134	158	144	128
Sm	25.20	24.70	15.10	22.50	19.70	19.90	21.50	18.50	19.80	15.20	20.20	18.70	23.00	21.20	18.00
Eu	6.89	6.33	4.31	5.76	5.27	5.11	5.50	4.82	5.14	4.05	5.24	4.91	5.98	5.52	4.79
Gd	17.90	17.00	10.40	15.70	12.70	12.50	14.50	11.80	12.50	10.10	13.10	11.80	15.50	14.00	11.50
Dy	7.88	7.60	4.70	7.86	5.13	5.68	7.13	5.33	5.26	4.53	5.94	5.27	7.05	6.47	5.15
Ho	1.23	1.18	0.74	1.23	0.82	0.90	1.13	0.84	0.83	0.73	0.99	0.84	1.12	1.03	0.84
Er	2.84	2.64	1.80	2.75	1.99	2.12	2.61	2.06	2.06	1.73	2.47	2.06	2.57	2.39	2.09
Yb	2.15	2.00	1.32	2.18	1.58	1.78	2.17	1.72	1.70	1.41	2.16	1.76	2.05	1.92	1.81
Lu	0.28	0.26	0.18	0.28	0.22	0.24	0.29	0.23	0.23	0.18	0.30	0.23	0.27	0.25	0.25
^{18}O	na	7.0	na	7.2	na	8.1	na	8.3	na	na	na	na	na	8.1	na
Sr_{400}	na	na	na	0.706135	na	na	na	0.705609	na	na	na	na	na	na	na
Nd_{400}	na	na	na	0.512002	na	na	na	0.511942	na	na	na	na	na	na	na

[a]Totals include SrO and BaO.

ships may be confirmed graphically by plotting the compositions of the relevant minerals (Table 2) on the Harker plots (Fig. 4). Extrapolation to low SiO_2 of tie-lines connecting the fields of syenites and monzodiorites intersect one connecting the fields of biotite and pyroxene analyses. Partial accumulation of this assemblage would leave monzogabbro cumulates. The effect of plagioclase and K-feldspar crystallisation is best seen in the Al_2O_3 and Na_2O plots where tie-lines between the analyses for these two minerals (perhaps with a minor amphibole component) intersect those connecting the fields of granites and syenites.

Least-squares mass-balance solutions (Bryan et al. 1969) for the monzodiorite to syenite and syenite to granite steps (Table 3) indicate that 50% fractionation of a biotite > clinopyroxene >>> titanite and apatite assemblage will drive monzodiorite to syenite, from where 60% fractionation of K-feldspar and plagioclase >> amphibole and apatite > titanite and magnetite will produce granite. Therefore, on the basis of smooth variations in major element oxide data, explicable in terms of removal of the observed minerals, the monzodiorites, syenites and granites may be cogenetic and related by crystal fractionation. Finally, the three samples that were identified on macroscopic and petrographic grounds as intimate hybrids between monzogabbro and syenite all fall on tie-lines between the fields of data for their parent end members. A simple binary mixing solution for these is presented in Table 3.

CCB 17	CCB 51	CCB 18	A 58	A 256	CCB 5a	CCB 12	CCB 10	CCB 13	A 37	CCB 6	CCB 7	CCB 9	CCB 8
Hybrids			Syenites							Granites			
64.80	57.07	58.23	58.39	60.18	62.34	62.44	62.78	63.82	65.62	69.63	70.31	70.62	70.66
15.60	14.33	15.39	18.16	17.08	16.25	15.91	17.05	15.82	16.94	16.08	15.51	15.57	15.44
1.00	0.85	0.75	0.70	0.57	0.64	0.65	0.51	0.64	0.52	0.31	0.36	0.38	0.36
6.32	5.34	5.60	4.48	3.50	3.77	4.22	3.64	4.05	3.32	2.25	1.69	1.90	1.80
0.10	0.12	0.15	0.09	0.06	0.07	0.06	0.08	0.07	0.05	0.05	0.02	0.02	0.02
6.17	3.98	3.64	1.63	1.77	1.53	1.62	0.78	1.51	0.95	0.79	0.68	0.69	0.66
6.25	6.05	5.44	2.98	2.91	3.54	3.21	2.44	3.33	1.58	1.04	1.02	1.44	1.35
2.89	6.09	3.91	5.54	4.46	5.99	4.82	5.20	5.78	4.58	5.27	5.61	4.09	4.11
4.76	3.36	4.87	5.07	5.48	4.48	4.92	5.18	4.70	6.09	4.65	4.13	5.01	5.07
0.51	0.75	0.65	0.45	0.39	0.31	0.32	0.21	0.31	0.17	0.11	0.12	0.11	0.09
1.44	1.57	1.44	1.31	2.67	1.34	0.87	1.20	0.29	0.42	0.26	0.57	0.35	0.57
100.19	100.10	100.60	99.27	99.55	100.92	99.70	99.62	100.90	100.68	100.69	100.23	100.37	100.32
70	116	72	120	79	90	70	79	75	63	139	122	100	101
na	1.9	na	2.6	2.1	na	na	na	0.7	0.5	2.7	na	na	1.1
1699	2144	2135	2118	2409	2704	2944	2278	2218	1694	1097	832	820	757
1315	3024	2482	1994	1943	3080	2772	2548	2843	2187	1121	979	862	856
18	22	23	21	16	27	25	24	26	17	8	10	6	4
12.0	24.0	29.0	53.6	37.3	15.0	17.0	52.0	15.5	23.2	27.6	25.0	22.0	23.6
na	5.7	na	11.2	6.2	na	na	na	4.6	5.0	4.4	na	na	4.8
249	354	360	553	407	335	343	523	331	373	209	241	213	205
na	8.6	na	14.9	12.7	na	na	na	7.6	8.4	5.2	na	na	5.6
15	22	24	37	20	21	23	37	22	21	13	7	5	6
na	1.8	na	3.1	1.8	na	na	na	2.3	2.3	1.9	na	na	1.6
99	69	65	57	43	52	57	43	55	36	23	20	23	20
166	133	112	2	29	16	20	0	19	3	6	6	7	9
27	21	21	22	17	22	26	40	30	25	54	47	49	73
101	32	33	5	26	8	10	1	7	3	4	2	2	2
19	10	14	14	4	18	21	21	26	13	5	2	8	6
95	78	110	83	68	42	51	58	37	69	47	27	52	51
73.3	153.0	175.0	166.0	135.0	139.0	132.0	197.0	147.0	123.0	63.7	65.7	57.8	49.4
141	301	343	297	261	272	259	360	268	223	116	103	90	85
15.1	28.8	31.1	25.2	24.2	25.8	25.3	30.3	25.8	20.9	10.7	10.5	9.5	8.4
52	105	112	83	82	89	87	100	88	68	33	32	29	26
7.11	14.40	15.00	10.40	9.03	12.20	11.70	11.30	11.40	8.71	4.16	4.28	3.77	3.29
1.99	3.68	3.78	2.83	2.47	3.21	3.10	2.99	3.02	2.40	1.18	1.15	0.97	0.82
5.19	9.45	9.43	6.98	6.02	8.20	7.80	7.20	7.79	5.68	2.71	2.88	2.36	2.07
3.48	4.87	4.65	3.92	3.31	4.93	4.79	4.28	4.83	3.30	1.67	1.80	1.22	1.15
0.63	0.81	0.79	0.70	0.57	0.89	0.85	0.76	0.87	0.59	0.31	0.33	0.21	0.20
1.76	2.09	2.05	1.84	1.43	2.43	2.33	2.02	2.38	1.60	0.87	0.86	0.57	0.50
1.79	1.97	1.90	1.85	1.41	2.48	2.31	2.14	2.46	1.67	0.92	0.87	0.50	0.47
0.25	0.27	0.27	0.28	0.20	0.35	0.33	0.31	0.36	0.24	0.14	0.13	0.07	0.07
na	8.7	na	9.3	9.1	na	na	na	9.7	9.3	10.2	na	na	9.8
na	0.707200	na	na	0.706108	na	na	na	na	na	0.707350	na	na	na
na	0.511932	na	na	0.511908	na	na	na	0.511848	na	0.511857	na	na	na

Further evidence for the proposed genetic relationship between the three main magmas may be seen in the close similarity of many trace element ratios. These are shown in Fig. 5, on multielement chondrite-normalised plots. The close coherence of the patterns is immediately apparent. All share the general increase in normalised abundances towards the left (i.e. those elements which are most incompatible with the minerals in normal mantle peridotite) and persistent troughs at the high field-strength elements Ti and Nb, Ta. Both these are characteristics of subduction-related magmas (see also Thompson and Fowler 1986). In detail, however, many progressive variations in interelement ratios may be identified. Perhaps the most eye-catching is fractionated Ba/Rb in the granites (Figs. 5A, D; 6A). The Sr trough present in the monzogabbros and monzodiorites is lost in the syenites and granites (Fig. 5B, C, D) and can be monitored by falling Ce/Sr (Fig. 6B). The small P trough in the monzodiorites and monzogabbros (Fig. 5B, though not all – those with small peaks may contain some cumulus apatite) deepens progressively throughout the evolution (increasing Nd/P_2O_5 - Fig. 6C), concurrent with a severe fractionation of the Sm/Zr ratio (Fig. 5B, C, D; 6D). The progressive development of concave-

Table 2 Selected mineral major element data for the Ach'Uaine Hybrid appinites

	Feldspars				
	CCB6p1	CCB6k1	CCB10p1	CCB10k1	LYD1p1
SiO_2	65.46	63.65	66.40	64.60	66.78
Al_2O_3	21.62	17.90	21.62	18.15	19.91
FeO	0.00	0.04	0.12	0.04	0.07
CaO	3.04	0.00	2.49	0.00	1.12
Na_2O	9.72	1.05	9.24	1.23	10.20
K_2O	0.17	15.68	0.30	14.88	0.12
BaO	0.00	0.42	0.04	0.48	0.00
Total	100.01	98.74	100.21	99.38	98.20
An	14.60	0.00	12.72	0.00	5.70
Ab	84.41	9.25	85.44	11.18	93.60
Or	0.98	90.76	1.84	88.82	0.70
	Biotites				
	LYD1b1	LYD1b2	CCB6b1	CCB6b2	CCB15b1
SiO_2	40.89	40.39	38.17	38.13	39.19
TiO_2	2.03	2.20	2.65	2.69	1.98
Al_2O_3	13.33	13.30	15.53	15.07	14.14
Cr_2O_3	0.00	0.14	0.10	0.09	0.03
FeO	14.65	14.18	19.45	19.71	15.47
MnO	0.15	0.15	0.59	0.56	0.15
MgO	16.56	16.41	10.52	10.78	14.85
CaO	0.00	0.00	0.01	0.00	0.00
Na_2O	0.06	0.07	0.09	0.07	0.05
K_2O	8.64	8.94	9.79	9.68	9.48
Total	96.31	95.78	96.90	96.77	95.34
Total + F	96.81	96.26	97.58	97.48	95.95
X_{ann}	0.31	0.30	0.44	0.45	0.33
X_{phlog}	0.62	0.62	0.43	0.43	0.57
F	0.50	0.48	0.68	0.71	0.61
	Amphiboles			**Pyroxenes**	
	CCB10a1	CCB10a2		LYD1px1	CCB15px1
SiO_2	45.89	52.92		51.09	51.66
TiO_2	0.86	0.35		1.01	0.61
Al_2O_3	7.98	4.09		2.01	3.12
Cr_2O_3	0.00	0.00		0.00	1.17
FeO	17.50	11.38		6.27	3.97
MnO	0.88	0.31		0.24	0.11
MgO	11.32	16.13		13.70	15.15
CaO	11.07	11.76		22.13	22.06
Na_2O	1.60	1.27		1.08	0.82
K_2O	1.11	0.44		0.00	0.00
Total	98.20	98.66		100.06	98.66
X_{HbFe}	0.46	0.28	Ca	0.48	0.47
X_{HbMg}	0.54	0.72	Mg	0.41	0.45
Mg#	52.32	71.07	Fe	0.11	0.07
			Mg#	78.94	86.86

upward curvature in the heavy REE patterns (Fig. 6E) can be defined by the Dy/Yb ratio, which is similar in the monzodiorites and monzogabbros (ca. 3–4), but has fractionated significantly in the syenites and granites (ca. 2, Fig. 6F).

Such ratio variations within the suite are explicable in terms of crystal-liquid equilibration between the early-forming crystals and the evolving magma. For example, apatite euhedra are ubiquitous in all the rocks, such that it represents the major phosphate host throughout the suite. The deepening P trough is therefore consistent with its progressive removal into apatite. Similarly, titanite is a common accessory phase and may be responsible, at least in part, for the persistently falling Ti. The affinity of apatite and titanite for middle REE is well documented (Fujimaki 1986; Green and Pearson 1986), as substitutions into the Ca site. Apatite data show significant LREE concentrations (La_2O_3 up to 0.27 wt%, Ce_2O_3 up to 0.53 wt%, Nd_2O_3 up to 0.33 wt%), with a progressive decline in total REE content from monzodiorite through syenite to granite. Figure 6 (G and H) show P_2O_5 and TiO_2 against the Dy/Yb monitor of the heavy REE curvature. The strong positive correlations are consistent with the removal of middle REE into separating apatite and titanite throughout the evolution from monzodiorite through syenite to granite. Accessory allanite (early falling Ce/Sr) is probably also involved, but limited Zr variation (resulting in severe Sm/Zr and Zr/Ti fractionation) restricts the involvement of zircon. It is well established that zircon saturation is retarded in alkaline magmas, and accessory zircon is most abundant in the granite extreme.

Thus, the elemental variations between the monzogabbros, monzodiorites, syenites and granites may be integrated with petrographic observations and mineral chemistry into an evolutionary scheme dominated by

Table 3 Least-squares mass-balance models of Ach'Uaine Hybrid appinite evolution. CCB1 monzodiorite produces CCB10 syenite by 50.6% fractionation of biotite (0.504) + clinopyroxene (0.359) + titanite (0.073) + apatite (0.064); sum^2 of residuals = 0.045. CCB10 syenite produces CCB9 granite by 61.1% fractionation of plagioclase (0.466) + K feldspar (0.393) + amphibole (0.083) + magnetite (0.018) + apatite (0.011); sum^2 of residuals = 0.038. CCB5i as a mixture of CCB1 monzodiorite and CCB5a syenite. 46.3% CCB1 + 53.7% CCB5a; $sum^2$of residuals = 0.717. Note that SiO_2 and Al_2O_3 have been weighted by factors of 0.4 and 0.5 respectively

	CCB10	CCB1 Obs	CCB1 Calc	Diff
SiO_2	64.39	52.88	52.99	–0.04
TiO_2	0.52	1.70	1.73	–0.03
Al_2O_3	17.49	12.93	13.02	–0.04
FeO	3.36	6.78	6.76	0.02
MnO	0.08	0.14	0.10	0.04
MgO	0.80	7.62	7.64	–0.02
CaO	2.50	8.36	8.31	0.05
Na_2O	5.31	2.89	2.75	0.14
K_2O	5.33	5.29	5.18	0.11
P_2O_5	0.22	1.41	1.48	–0.07
	CCB9	CCB10 Obs	CCB10 Calc	Diff
SiO_2	70.88	64.39	64.37	0.00
TiO_2	0.38	0.52	0.59	–0.07
Al_2O_3	15.63	17.49	17.60	–0.06
FeO	1.72	3.36	3.36	0.00
MnO	0.02	0.08	0.06	0.02
MgO	0.69	0.80	0.88	–0.08
CaO	1.45	2.50	2.51	0.09
Na_2O	5.03	5.31	5.28	0.03
K_2O	4.10	5.33	5.31	0.02
P_2O_5	0.11	0.22	0.33	–0.12
	CCB1	CCB5i Obs	CCB5i Calc	CCB5a	Diff
SiO_2	52.88	58.59	58.71	63.26	–0.05
TiO_2	1.70	0.87	1.14	0.65	–0.27
Al_2O_3	12.93	14.71	14.91	16.49	–0.10
FeO	6.78	4.93	5.01	3.44	–0.08
MnO	0.14	0.12	0.10	0.07	0.02
MgO	7.62	4.09	4.38	1.55	–0.29
CaO	8.36	6.21	5.83	3.59	0.39
Na_2O	2.89	3.45	3.80	4.55	–0.35
K_2O	5.29	6.25	5.47	6.08	0.52
P_2O_5	1.41	0.77	0.83	0.31	–0.06

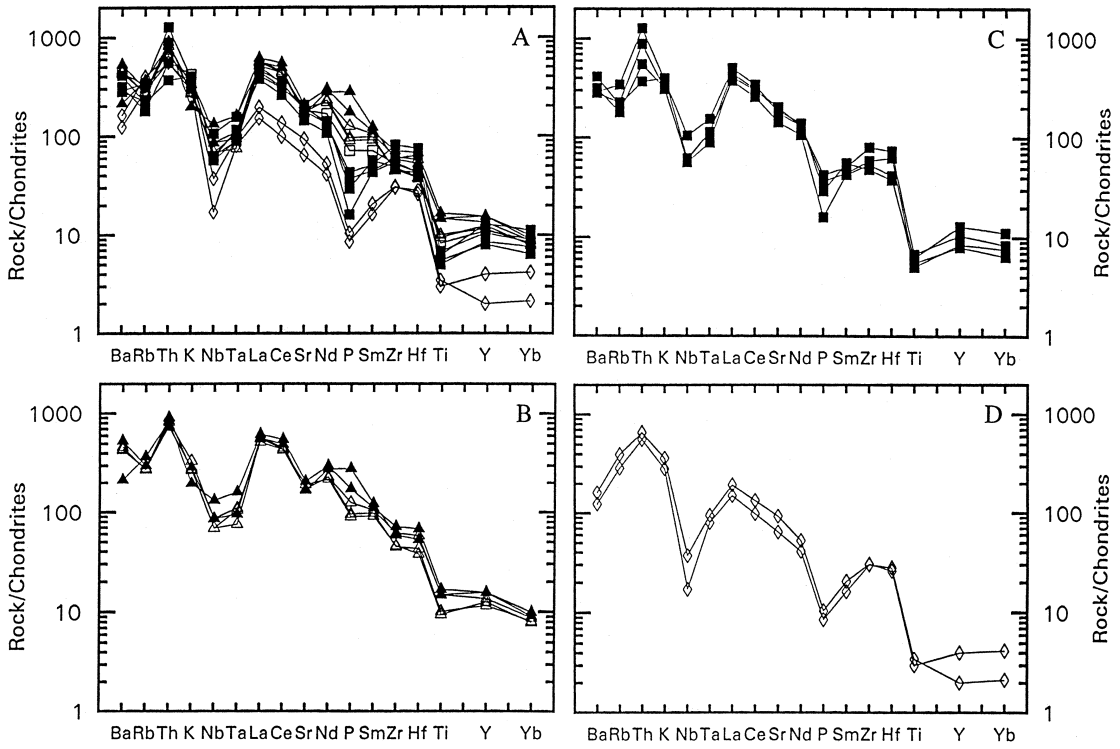

Fig. 5A–D Chondrite-normalised multielement plots for the Ach'Uaine Hybrid Appinites (values and order after Thompson 1982). Symbols as in Fig. 4. **A** Representative data for the whole suite. **B** Monzogabbros and monzodiorites. **C** Syenites. **D** Granites

crystal fractionation. The macroscopic and microscopic evidence for the presence of several discrete magmas further requires that this proceeded in a compositionally-complex, evolving magma chamber. Monzodiorite was the mantle-derived component, which coexisted with syenite and probably also granitic residua. The solutions obtained from major element modelling do not require significant crustal input, but such silica oversaturation trends towards granite are often accompanied by isotopic evidence for crustal involvement (Foland et al. 1993).

Isotopes

Three isotope systems were studied to provide further constraints on the extent of crustal interaction during magma evolution. $\delta^{18}O$ varies from < + 7‰ to > + 10‰, $^{87}Sr/^{86}Sr_{400}$ from < 0.7057 to > 0.7073 and $^{143}Nd/^{144}Nd_{400}$ from 0.51185 to > 0.51200 (Table 1). This range of variation in all three systems rules out closed system evolution and confirms that significant crustal contamination occurred. Figure 7A displays the data as deviations from Bulk Earth at 400 Ma. Contemporary depleted mantle reservoirs occupy the top left quadrant, sub-continental lithospheric mantle (SCLM: Lorne and Roag) and the two likely crustal contaminants (Lewisian gneisses at amphibolite or granulite facies, and Moine metasediments) occupy parts of the lower two quadrants, as shown. The parental monzodiorite had $^{87}Sr/^{86}Sr$ ca. 0.7056, $^{143}Nd/^{144}Nd$ ca. 0.51195 and $\delta^{18}O$ ca. + 8‰, for which there are several petrogenetic options. The presence of an "enriched lithospheric keel" under N and NW Scotland has been well documented in recent isotopic studies of xenolith suites (Holden et al. 1987 , Halliday et al. 1993), or invoked in contemporary accounts of Caledonian magmatism (Thirlwall 1982). The heterogeneity of this SLCM reservoir is clear from the diagram (Lorne and Roag on Fig. 7A), and large contributions to the Ach'Uaine magmas are possible. Significantly, $\delta^{18}O$ in the monzodiorites is high relative to the accepted range of mantle values (+ 5.5 to + 6‰), consistent with some early contamination in the lower crust, unless high $\delta^{18}O$

Fig. 6A–H Progressive interelement ratio fractionation. Symbols as in Fig. 4. **A** Ba/Rb vs SiO_2 showing a range of values in monzogabbros, monzodiorites and syenites, suddenly fractionated in the granites. **B** Ce/Sr vs SiO_2 to monitor Sr anomaly seen on Fig. 5, showing steady gentle decrease. **C** Nd/P_2O_5 vs SiO_2, increasing throughout the fractionation as negative P anomaly (Fig. 5) develops. **D** Sm/Zr vs SiO_2 falling from monzodiorites and monzogabbros through syenites to granites. **E** Chondrite-normalised REE plot (Nakamura 1974) showing coherence of the suite but progressive development of concave-upward heavy REE curvature. **F** Dy/Yb vs SiO_2 to monitor heavy REE curvature. **G** Dy/Yb vs P_2O_5, both decreasing from monzogabbro through monzodiorite and syenite to granite as a result of apatite fractionation. **H** Dy/Yb vs TiO_2, showing a similar trend due to titanite fractionation

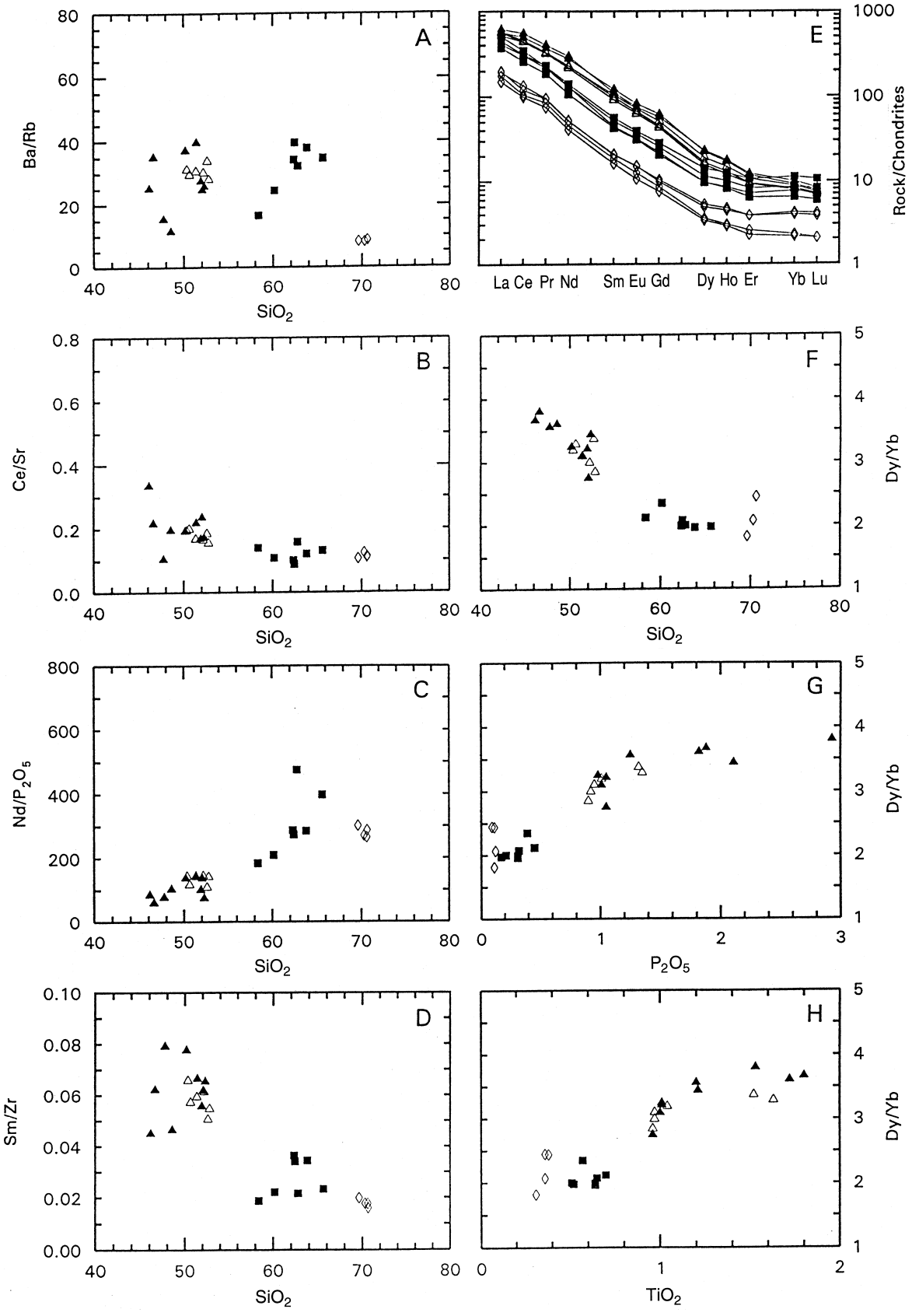
A
Ba/Rb
SiO2
B
Ce/Sr
SiO2
C
Nd/P2O5
SiO2
D
Sm/Zr
SiO2
E
Rock/Chondrites
La Ce Pr Nd Sm Eu Gd Dy Ho Er Yb Lu
F
Dy/Yb
SiO2
G
Dy/Yb
P2O5
H
Dy/Yb
TiO2

Fig. 6A–H

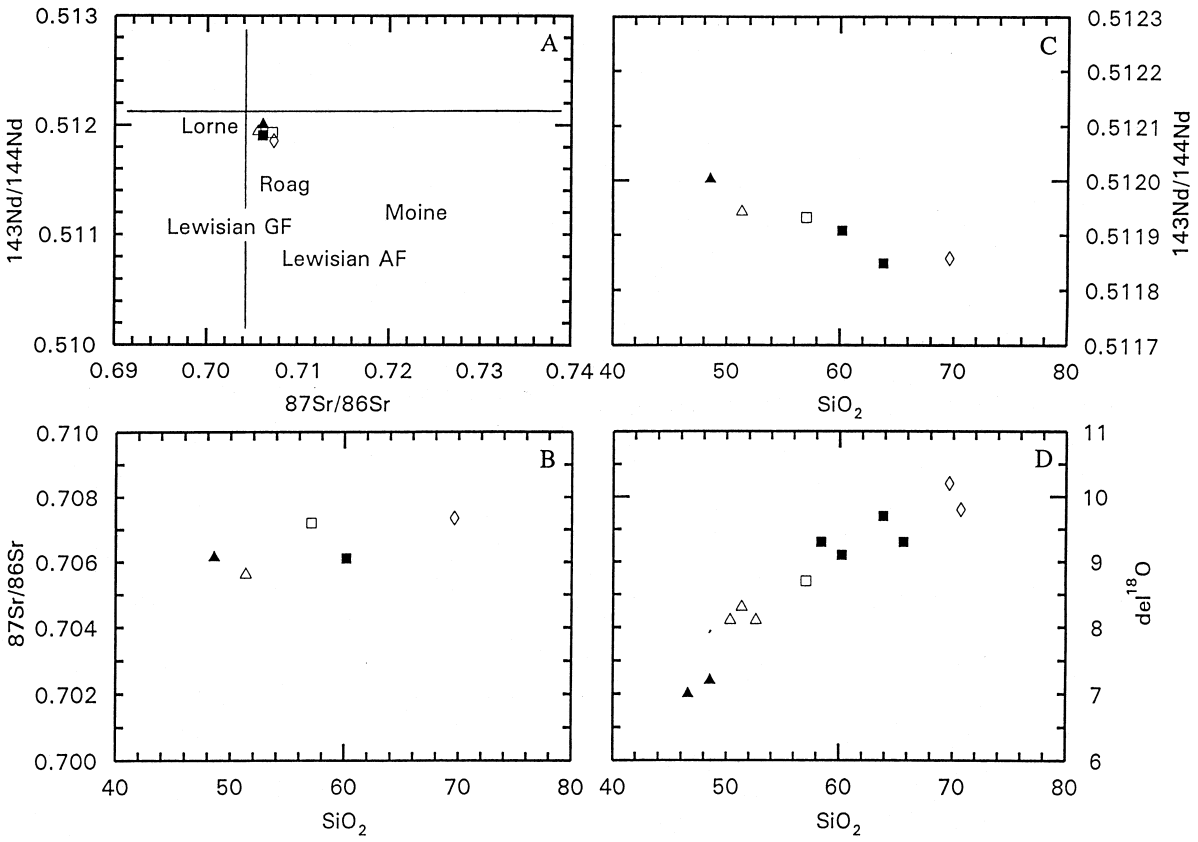

Fig. 7A–D Radiogenic and stable isotope data and their relationships with SiO_2. Symbols as in Fig. 4. **A** $^{143}Nd/^{144}$ Nd vs $^{87}Sr/^{86}Sr$ at 400Ma. Fields for Lewisian lower crust (granulite or amphibolite facies), Moine upper crust, subcontinental lithospheric mantle (Loch Roag xenoliths, Lorne source mantle) plotted, see text for sources. **B** $^{87}Sr/^{86}Sr$ vs SiO_2 (r = 0.71), **C** $^{143}Nd/^{144}Nd$ vs SiO_2 (r = 0.93), **D** $\delta^{18}O$ vs SiO_2 (r = 0.93). **B**, **C** and **D** all show strong correlations; r is the correlation coefficient

also characterises the lithospheric mantle.The proportion of material derived from contemporary depleted mantle would seem severely limited, but it is difficult to rule out unequivocally ca. 10% contamination of this with mid-upper crust to form the most primitive of the Ach'Uaine magmas. The syenites have uniformly higher $\delta^{18}O$ (+ 9.1 to + 9.7‰), more radiogenic $^{87}Sr/^{86}Sr$ at 0.7061 and less radiogenic $^{143}Nd/^{144}Nd$ averaging 0.51188. The granites extend this trend to the highest $\delta^{18}O$ values (+ 9.8 to + 10.2‰), most radiogenic $^{87}Sr/^{86}Sr$ (0.7074) and least radiogenic $^{143}Nd/^{144}Nd$ (0.51186). Extrapolation of the isotopic array thus defined intersects the fields of the two likely crustal reservoirs. Given the common presence of Moine xenoliths noted above, contamination of the acid differentiates with Moine seems probable, and is tested below.

Contamination mechanisms

Strong linear correlations between the radiogenic and stable isotope systems and silica (Fig. 7B,C,D) are consistent with binary mixing between the mantle-derived monzodiorite and the surrounding Moine metasediments or a felsic magma derived from them, similar to the hypothesis advanced by Harmon et al. (1984) for the production of British Caledonian Newer Granites in general. However, the elemental variations discussed above betray the significant control of crystal fractionation and rule out such a mechanism for progressive crustal input. Instead, the application of elemental and isotopic constraints requires crustal assimilation to be concurrent with crystal fractionation immediately prior to emplacement. It therefore seems reasonable to attempt to model the evolution of the magmas in terms of assimilation - fractional crystallisation (AFC) processes.

AFC trajectories for progressive contamination of the evolving magmas with the surrounding Moine metasediments are presented on $^{143}Nd/^{144}Nd$ vs Nd (Fig. 8A), $^{143}Nd/^{144}Nd$ vs $\delta^{18}O$ (Fig. 8B), $^{87}Sr/^{86}Sr$ vs Sr (Fig. 8C), and $^{87}Sr/^{86}Sr$ vs $\delta^{18}O$ plots (Fig. 8D). Two trends are plotted, in accord with the major element models above. Trend 1 represents ca. 50% fractionation dominated by biotite plus pyroxene, producing a syenitic daughter from a monzodiorite parent. Trend 2 represents further evolution of the syenite towards granite, controlled by ca. 60% feldspar removal. The closest fits to the data are then derived assuming a relatively low, but geologically-realistic ratio of contamination to fractionation rate of 0.2 (DePaolo 1981). Bulk dis-

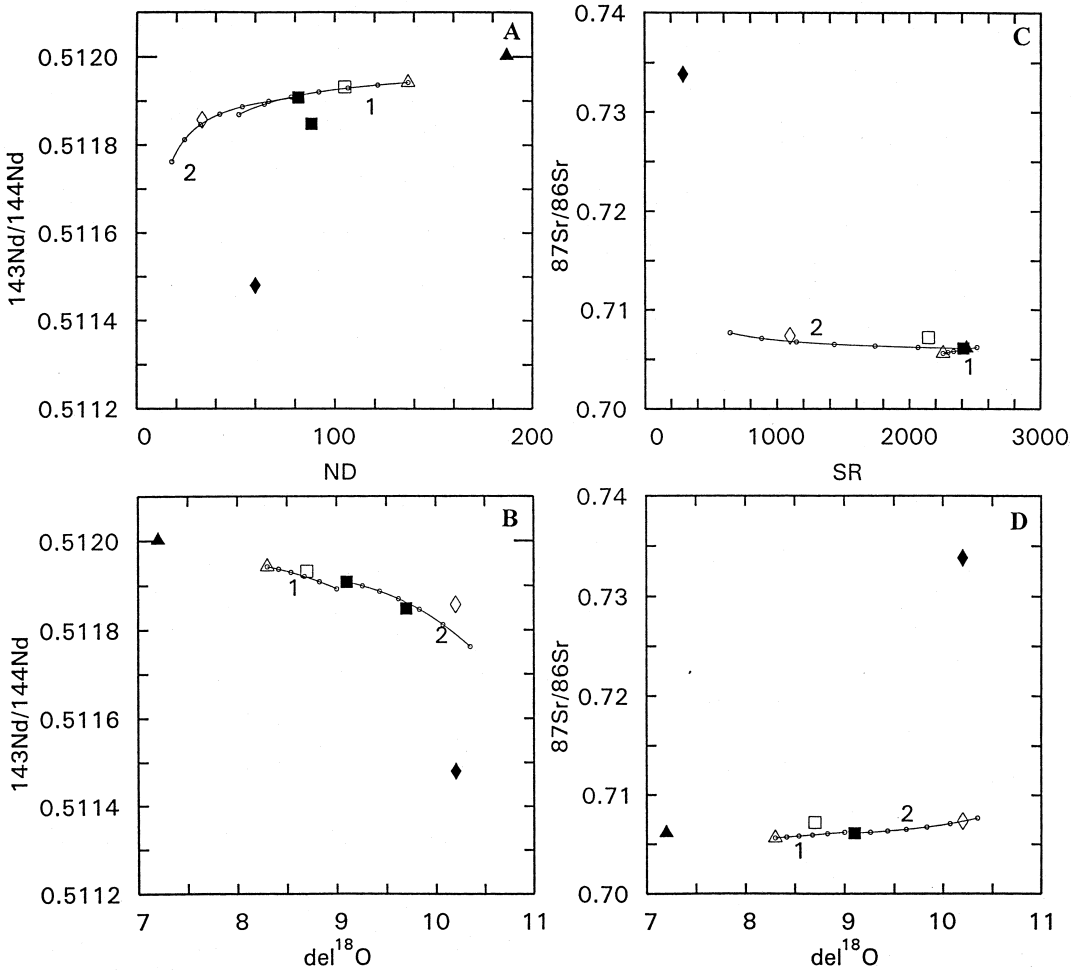

Fig. 8A–D Assimilation - fractional crystallisation isotope models with Moine metasedimentary rocks as contaminant. Symbols as in Fig. 4, plus *closed diamond* Moine (from Fowler 1988b, 1992). **A** $^{143}Nd/^{144}Nd$ vs Nd. **B** $^{143}Nd/^{144}Nd$ vs $\delta^{18}O$. **C** $^{87}Sr/^{86}Sr$ vs Sr. **D** $^{87}Sr/^{86}Sr$ vs $\delta^{18}O$. Two fractionation stages have been modelled. *Trend 1* 50% biotite plus pyroxene and accessories, with bulk distribution coefficients as follows: Sr = 0.7, Nd = 1.8. *Trend 2* 60% feldspar-dominated plus accessories, with Sr = 2.0, Nd = 2.5. For both trends, the ratio of assimilation rate to fractionation rate (R) = 0.2. For trend 1, Δ (= $\delta_{crystals}$ - δ_{melt}) has been set to –0.5, for trend 2 set to –1.0. *Tick marks* represent proportion of melt remaining, in 10% steps

tribution coefficients for Sr and Nd are noted in the figure caption, computed on the basis of mineral proportions in the least-squares major element models (Table 3). They are in accord with published data for the minerals concerned (Rollinson 1993) and in particular are within the ranges established for a compositionally-comparable alkali basalt to phonolite suite (Villemant et al. 1981). Figure 9 presents examples of similar AFC models on bivariate trace element plots, for samples that are believed to be close to liquid compositions (i.e. minus the monzogabbros, that are interpreted as having sometimes-large cumulus proportions). Given the difficulty in estimating the fractionating proportions of minor and accessory phases, and the uncertainty surrounding partition coefficient data for some of them, only elements that enter the main rock-forming minerals are used (alkali and alkaline earth metals, transition metals). Bulk distribution coefficients were estimated as before and are noted in the figure captions. Figure 9 (A, B) shows Rb and Ba vs Sr plots, on which the inflexions defined by tie lines joining the centres of the three fields of data (monzodiorites, syenites and granites), can be explained by the switch from pyroxene- and biotite-dominated fractionation (trend 1) to plagioclase and K-feldspar control (trend 2). Transition metal data (Fig. 9C,D) decrease steadily with fractionation, despite the predominance of feldspars in the syenite to granite step. This may be the result of significant magnetite involvement at this stage (see petrography, above), continuing to remove transition metals from the melt. It is clear from these diagrams that sensible AFC models adequately explain the elemental evidence for crystal fractionation and the isotopic evidence for crustal contamination, and require similar fractionating proportions to the quantitative major element models. Given these proportions, and the contamination to fractionation rate ratio (R) of 0.2, the additional crustal contribution required to derive syenite from the

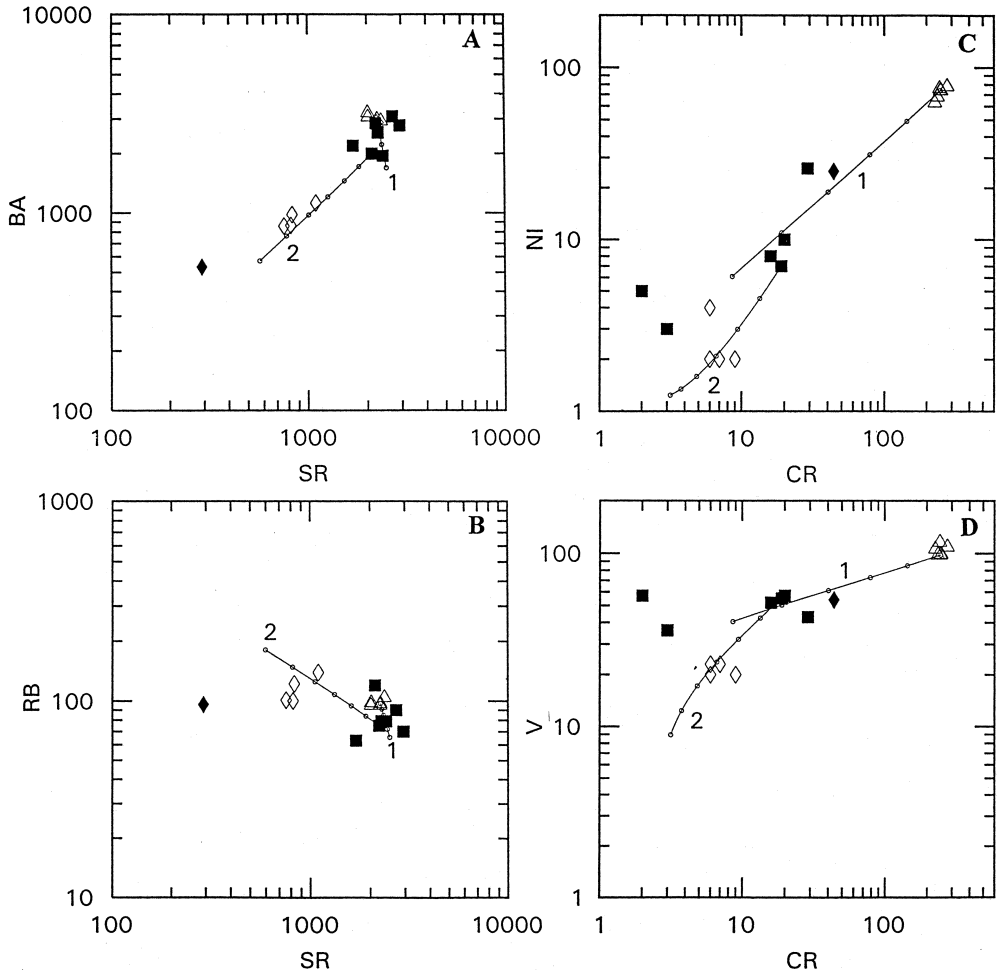

Fig. 9A–D Assimilation - fractional crystallisation element models. Symbols as in Fig. 4. Trends computed as for Fig. 8. **A** Ba vs Sr. **B** Rb vs Sr. **C** Ni vs Cr. **D** V vs Cr. Bulk distribution coefficients as follows: *trend 1* Sr = 0.7, Ba = 1.5, Rb = 1.5, Cr = 5.0, Ni = 4.0, V = 2.0; *trend 2* Sr = 2.0, Ba = 2.0, Rb = 0.2, Cr = 4, Ni = 5, V = 3. For both trends R = 0.2. *Tick marks* represent proportion of melt remaining, in 10% steps

monzodiorite may be as little as 10%, and that needed to produce granite only some 20–25%. Therefore, the high Ba-Sr style of granitoid magmatism represented by these rocks includes a major juvenile component derived from subcontinental lithospheric mantle, which has been severely underestimated in the past.

Discussion

Field relationships and textural evidence presented above argue for the coexistence of discrete lamprophyric (monzodiorite) and syenitic magmas. Although contemporaneity of these and the cross-cutting granite sheets is precluded by the field relationships, petrographic and geochemical evidence suggest a close genetic relationship. The low silica contents and high MgO associated with high transition metal abundances in the monzodiorites are consistent with mantle derivation, and high Cr/Ni suggests significant high-pressure fractionation involving olivine. However, the absence of olivine in even the most mafic compositions suggests prolonged residence at upper crustal pressures where reaction to mica would occur (Esperança and Holloway 1987). Clear evidence of the controlling role of crystal fractionation is given by systematic changes in interelement ratios closely related to the observed crystallisation sequence of the magmas. Two trends explain all the main features of the data. Early fractionation of the lamprophyric magma was driven by the crystallisation and separation of calcic clinopyroxene, biotite, apatite and titanite, producing broadly silica-saturated syenites by approximately 50% fractionation. The unusual trend of decreasing REE abundances is a consequence of the early crystallisation of the minor minerals. Even during this early stage there is unequivocal isotopic evidence of minor crustal input. Further evolution of the syenitic magma to granite involved approximately 60% fractionation of plagioclase, K-feldspar, magnetite and an array of minor phases (apatite, titanite, allanite and eventually zircon), with continued contamination by small amounts of Moine metasediment recorded in the

stable and radiogenic isotope systematics. These results are in accord with recent discussions of phase equilibria constraints (Foland et al. 1993; Landoll et al. 1994), and direct observations on related magmas in which minor contamination produced syenite (Thirlwall and Burnard 1990) and significant contamination produced granite (Fowler 1992). However, in the system studied here, the crustal input required to proceed to a silica-oversaturated terminus is small (< 25%), since low ratios of contamination to fractionation rate (ca. 0.2) are required.

The implications of this study to the topic of granite genesis are considerable. As pointed out by Fowler (1988a), the lamprophyres, syenites and granites of the Ach'Uaine appinites have direct compositional analogues in the discrete lamprophyre dykes, syenite and granite plutons of the Caledonian orogen. The comparability of elemental data for the Ach'Uaine appinites and the Rogart and Glenelg-Ratagain Newer Granites is remarkable (Fig. 10). All the elemental peculiarities of the Northern Highland Newer Granites are present in the Ach'Uaine appinite data (e.g. high Ba, Sr; high LREE but total REE abundances that fall with fractionation, lack of pronounced negative Eu anomalies in true granites). Closely associated with each granitoid pluton are fragments or facies of mafic, appinitic material. It follows that the model constructed for the fractionation of the Ach'Uaine monzodiorites may also be applicable to the generation of the local Caledonian Newer Granites. Although at Ach'Uaine the abundance of mafic rocks is sufficient to account for the volume of contemporaneous felsic differentiates in situ, relative volumetric relationships between mantle-derived mafic parent and daughter granite in the fully-developed granitoid plutons have been seen as irreconcilable with a dominant role for crystal fractionation. Nevertheless, the temporally- and spatially-associated Caledonian appinites are compositionally viable as mantle-derived components. They are often enriched in clinopyroxene and biotite to produce scyelites and related ultramafic rocks, which may therefore represent the cumulates required for appinite to syenite evolution (trend 1 above). Further crystal fractionation, mixing and assimilation involving accumulation of felsic cumulates (trend 2 above) into evolving granitoid magmas would produce the broad spectrum of diorites, granodiorites and granites observed in Caledonian Newer Granite plutonism. Thus, the distinctive HiBaSr trace element characteristics (Tarney and Jones 1994) derive from the mantle component, and not the continental crust. However, comparative radiogenic isotope data for related magmas in the Northern Highlands suggest that despite the clear elemental kinship this mantle source was markedly heterogeneous. For example, the radiogenic Sr and unradiogenic Nd isotopic ratios of the mafic Ach'Uaine magmas require time-integrated LILE and LREE enrichment, similar to that present in the Loch Roag xenolith suite thought to represent sub-Lewisian lithospheric mantle (Menzies and Halliday 1988). Late Caledonian minettes from the Northern Highlands (Canning et al. 1996) require similar or even more extreme enrichment. On the other hand, a significant component of less-enriched mantle is required in the Borralan syenites (Thirlwall and Burnard 1990), whereas a component of depleted mantle is required in that at Glen Dessarry (Fowler 1992). Therefore, in this classic area of HiBaSr granitoid magmatism, a complex array of mantle materials contributed to the distinctive geochemistry, which was enhanced but not significantly modified by extensive crystal fractionation and minor crustal contamination.

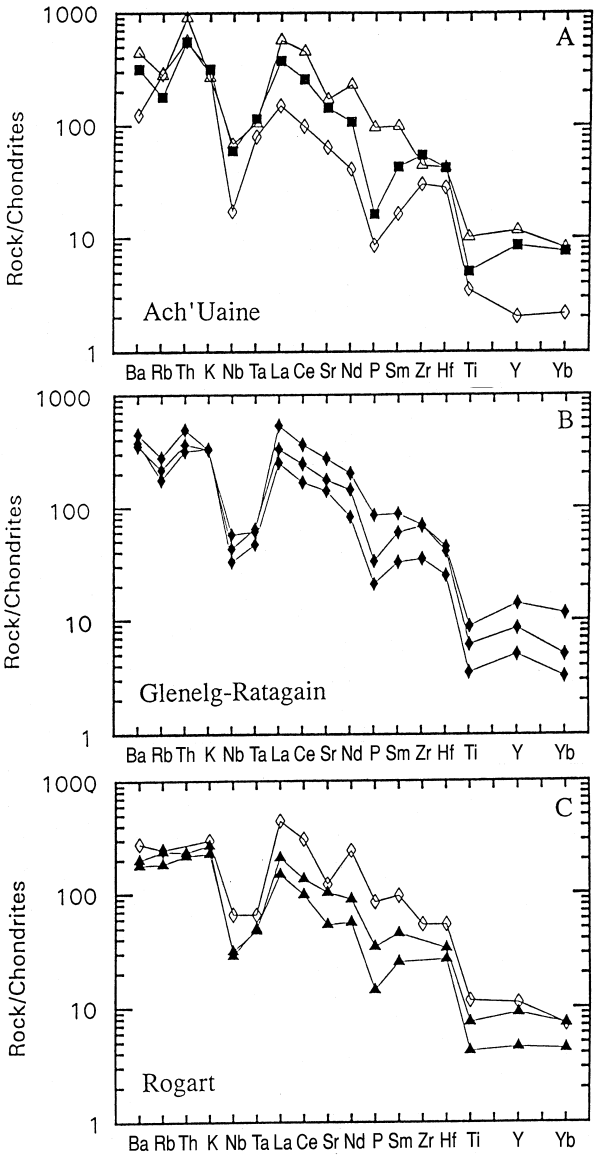

Fig. 10A–C Comparative chondrite-normalised multielement plots for **A** Ach'Uaine Hybrid Appinites (this work). **B** Glenelg - Ratagain diorite - syenite - adamellite (Thompson and Fowler 1986). **C** Rogart appinite - granodiorite - granite (MBF and PJH unpublished)

Acknowledgements We are grateful to many colleagues for their help during the conduct of this research. The isotopic analyses were

performed at the NERC Isotope Geosciences Laboratory, under the particular guidance of Peter Greenwood and Jane Evans. Baruch Spiro and Bob Pankhurst are thanked for their encouragement and advice, and Richard D'Lemos and Gordon Watt constructively criticised an earlier draft. Two reviewers are thanked for full and perceptive criticism, which helped to improve the manuscript.

References

Allan JF, Carmichael ISE (1984) Lamprophyric lavas in the Colima graben, SW Mexico. Contrib Mineral Petrol 88: 203–16

Bowes DR , McArthur AC (1976) Nature and genesis of the appinite suite. Kristalinikum 12: 31–46

Bryan WB, Finger LW, Chayes F (1969) Estimating proportions in petrographic mixing equations by least squares approximation. Science 163: 926–27

Canning JC, Henney PJ, Morrison MA, Gaskarth JW (1996) Geochemistry of late Caledonian minettes from northern Britain: implications for the Caledonian sub-continental lithospheric mantle. Mineral Mag 60: 221–236

Clayton RN, Mayeda TK (1963) The use of bromine pentafluoride in the extraction of oxygen from oxides and silicates for isotopic analysis. Geochim Cosmochim Acta 27: 43–52

D'Lemos RS (1992) Magma-mingling and melt modification between granitic pipes and host diorite, Guernsey, Channel Island. J Geol Soc London 149: 709–720

DePaolo DJ (1981) Trace element and isotopic effects of combined wallrock assimilation and fractional crystallisation. Earth Planet Sci Lett 53: 189–202

Esperança S, Holloway JR (1986) The origin of the highK latites from Camp Creek, Arizona: constraints from experiments with variable fO_2 and aH_2O. Contrib Mineral Petrol 93: 504–512

Esperança S, Holloway JR (1987) On the origin of some mica-lamprophyres: experimental evidence from a mafic minette. Contrib Mineral Petrol 95: 207–216

Foland KA, Landol JD, Henderson CMB, Jiangfeng C (1993) Formation of cogenetic quartz and nepheline syenites. Geochim Comochim Acta 75: 697–704

Fowler MB (1988a) Ach'uaine hybrid appinite pipes: evidence for mantle-derived shoshonitic parent magmas in Caledonian granite genesis. Geology 16: 1026–1030

Fowler MB (1988b) Elemental evidence for crustal contamination of mantle-derived Caledonian syenite by metasediment anatexis and magma mixing. Chem Geol 69: 1–16

Fowler MB (1992) Elemental and O-Sr-Nd isotope geochemistry of the Glen Dessarry syenite, NW Scotland. J Geol Soc London 149: 209–220

Fujimaki H (1986) Partition coefficients of Hf, Zr and REE between zircon, apatite and liquid. Contrib Mineral Petrol 94: 42–45

Gibson SA, Thompson RN, Leat PT, Morrison MA, Hendry GL, Dickin AP, Mitchell JG (1993) Ultrapotassic magmas along the flanks of the Oligo-Miocene Rio Grande rift, USA: monitors of the zone of lithospheric mantle extension and thinning beneath a continental rift. J Petrol 34: 187–228

Green TH, Pearson NJ (1986) Rare-earth element partitioning between sphene and coexisting silicate liquid at high pressure and temperature. Chem Geol 55: 105–119

Halliday AN, Dickin AP, Hunter RN, Davies GR, Dempster TJ, Hamilton PJ, Upton BJG (1993) Formation and composition of the lower continental crust: evidence from Scottish xenolith suites. J Geophys Res 98: B1 581–607

Hamidullah S, Bowes DR (1987) Petrogenesis of the appinite suite, Appin district, western Scotland. Acta Univ Carol Geol 4: 295–396

Harmon RS, Halliday AN, Clayburn JAP, Stephens WE (1984) Chemical and isotopic systematics of the Caledonian intrusions of Scotland and northern England: a guide to magma source regions and magma-crust interaction. Phil Trans R Soc London A310: 709–742

Holden P, Halliday AN, Stephens WE (1987) Neodymium and strontium isotope content of microdioritic enclaves points to mantle input to granitoid production. Nature 330: 53–56

Holden P, Halliday AN, Stephens WE, Henney PJ (1991) Chemical and isotopic evidence for major mass transfer between mafic enclaves and felsic magma. Chem Geol 92: 135–152

Landoll JD, Foland KA, Henderson CMB (1994) Nd isotopes demomstrate the role of contamination in the formation of coexisting quartz and nepheline syenites at the Abu Khruq Complex, Egypt. Contrib Mineral Petrol 117: 305–329

Leat PT, Thompson RN, Morrison MA, Hendry GL, Trayhorn SC (1987) Geodynamic significance of post-Variscan intrusive and extrusive potassic magmatism in SW England. Trans R Soc Edinburgh: Earth Sci 77: 349–60

MacGregor AG, Kennedy QC (1932) The Morvern-Strontian 'granite'. Geol Surv GB Summ Progr for 1931 II: 105–19

Marshall LA, Sparks RSJ (1984) Origin of some mixed-magma and net-veined ring intrusions. J Geol Soc London 141: 171–182

Menzies MA, Halliday A (1988) Lithospheric domains beneath the Archaean and Proterozoic crust of Scotland. J Petrol Spec Lithosphere Issue: 275–302

Middlemost EAK (1994) Naming materials in the magma/igneous rock system. Earth-Sci Rev 37: 215–224

Morrison GW (1980) Characteristics and tectonic setting of the shoshonite rock association. Lithos 13: 97–108

Nakamura N (1974) Determination of REE, Ba, Fe, Mg, Na and K in carbonaceous and ordinary chondrites. Geochim Cosmochim Acta 38: 757–775

Pitcher WS (1993) The nature and origin of granite. Chapman and Hall, London

Platten IM (1991) Zoning and layering in the diorites of the Scottish Caledonian appinite suite. Geol J 26: 329–348

Read HH, Phemister J, Ross G (1926) Geology of Strath Oykell and lower Loch Shin. Geol Surv GB Mem Geol Surv Scot: 154–166

Righter K, Carmichael ISE (1996) Phase equilibria of phlogopite lamprophyres from western Mexico: biotite-liquid equilibria and *P-T* estimates for biotite-bearing igneous rocks. Contrib Mineral Petrol 123: 1–21

Rock NMS (1984) Nature and origin of calc-alkaline lamprophyres: minettes, vogesites, kersantites and spessartites. Trans R Soc Edinburgh: Earth Sci 74: 193–227

Rock NMS (1991) Lamprophyres. Blackie, Glasgow

Rock NMS, Hunter RH (1987) Late Caledonian dyke-swarms of northern Britain: spatial and temporal intimacy between lamprophyric and granitic magmatism around the Ross of Mull pluton, Inner Hebrides. Geol Rundsch 76: 805–826

Roden MF (1981) Origin of coexisting minette and ultramafic breccia, Navajo volcanic field. Contrib Mineral Petrol 77: 195–206

Rollinson HR (1993) Using geochemical data: evaluation, presentation, interpretation. Longman, London

Stephens WE, Halliday AN (1984) Geochemical contrasts between Late Caledonian granitoid plutons of northern, central and southern Scotland. Trans R Soc Edinburgh: Earth Sci 75: 259–273

Stephens WE, Holden P, Henney PJ (1991) Microdioritic enclaves within the Scottish Caledonian granitoids and their significance for crustal magmatism. In: Didier J, Barbarin B (eds) Enclaves and granite petrology, Elsevier, Amsterdam, pp 125–133

Stille P, Oberhansli R, Wenger-Schenk K (1989) Hf-Nd and trace element constraints on the genesis of alkaline and calk-alkaline lamprophyres. Earth Planet Sci Lett 96: 209–219

Tarney J, Jones CE (1994) Trace element geochemistry of orogenic igneous rocks and crustal growth models. J Geol Soc London 151: 855–868

Thirlwall MF (1982) Systematic variation in chemistry and Nd-Sr isotopes across a Caledonian calc-alkaline volcanic arc: implications for source materials. Earth Planet Sci Lett 58: 27–50

Thirlwall MF, Burnard P (1990) Pb-Sr-Nd isotope evidence and chemical study of the origin of undersaturated and over-

saturated shoshonitic magmas from the Borralan pluton, Assynt, NW Scotland. J Geol Soc London 147: 259–269
Thompson RN (1982) Magmatism of the British Tertiary Volcanic Province. Scott J Geol 18: 50–107
Thompson RN, Fowler MB (1986) Subduction-related shoshonitic and ultrapotassic magmatism: a study of Siluro-n-Ordovician syenites from the Scottish Caledonides. Contrib Mineral Petrol 94: 507–522
Thompson RN, Leat PT, Dickin AP, Morrison MA, Hendry GL, Gibson SA (1989) Strongly potassic mafic magmas from lithospheric mantle sources during continental extension and heating: evidence from Miocene minettes of nortwest Colorado, USA. Earth Planet Sci Lett 98: 139–153
Vernon RH (1991) Interpretation of microstructures of microgranitoid enclaves. In: Didier J, Barbarin B (eds) Enclaves and granite petrology, Elsevier, Amsterdam, pp 277–291
Villemant B, Jaffrezic H, Joron J-L, Treuil M (1981) Distribution coefficents of major and trace elements: fractional crystallisation in the alkali basalt series of Chaine des Puys (Massif Central, France). Geochim Cosmochim Acta 45: 1997–2016
Wallace P, Carmichael ISE (1989) Minette lavas and associated leucitites from the Western Front of the Mexican Volcanic Belt: petrology, chemistry and origin. Contrib Mineral Petrol 103: 470–492
Walsh JN, Buckley F, Barker J (1981) The simultaneous determination of rare earth elements in rocks using inductively coupled plasma-source spectrometry. Chem Geol 33: 141–153
Watson EB (1982) Melt infiltration and magma evolution. Geology 10: 236–240
Wright AE, Bowes DR (1979) Geochemistry of the appinite suite. In: Harris AL, Holland CH, Leake BE (eds) The Caledonides of the British Isles reviewed. Geol Soc London Spec Pub 8: 699–704
Wyman DA, Kerrich R (1993) Archean shoshonitic lamprophyres of the Abitibi subprovince, Canada: petrogenesis, age and tectonic setting. J Petrol 34: 1067–1109
Wyman DA, Kerrich R, Sun M (1995) Noble metal abundances of late Archean (2.7 Ga) accretion-related shoshonitic lamprophyres, Superior Province, Canada. Geochim Cosmochim Acta 59: 47–57